Self-Assembly, Molecular Packing, and Electron Transport in n-Type Polymer Semiconductor Nanobelts

Alejandro L. Briseno,[†] Stefan C. B. Mannsfeld,[‡] Patrick J. Shamberger,[§] Fumio S. Ohuchi,[§] Zhenan Bao,[‡] Samson A. Jenekhe,*[,†,||] and Younan Xia*[,†]

Department of Chemistry, Department of Materials Science & Engineering, and Department of Chemical Engineering, University of Washington, Seattle, Washington 98195, and Department of Chemical Engineering, Stanford University, Stanford, California 94305

Received April 13, 2008

We have found that poly(benzobisimidazobenzophenanthroline) (BBL) nanobelts can be prepared by a simple high-yield, solution-phase process, which enables dispersions of the nanobelts in a large number of solvents including environmentally benign solvents such as methanol and water. Characterization of the nanobelts by transmission electron and atomic force microscopies, electron diffraction, and X-ray diffraction showed that the BBL polymer chains are oriented parallel to the long axis of each nanobelt. This unique packing motif is unlike the reported packing of polymer chains in other nanostructures, such as poly(3-hexylthiophene) nanowires, where the polymer backbone packs face-to-face along the nanowire direction. This unusual molecular packing in BBL nanobelts is explained by the rather strong intermolecular interactions, which are a result of the rigid and planar polymer chains. We investigated electron transport in single nanobelts and nanobelt networks via field-effect transistors and observed mobilities up to $\sim 7 \times 10^{-3}$ cm^2 V^{-1} s^{-1} and on/off current ratios of $\sim 1 \times 10^4$. The n-channel nanobelt transistors showed stability and repeatability in air for more than 6 months, which is the most stable among current n-channel polymer transistors. These results demonstrate that the BBL nanobelts are promising for organic electronics and nanoelectronics.

Introduction

One-dimensional (1D) organic semiconductor nanostructures such as nanowires and nanobelts are of fundamental interest for understanding structure−property relationships in conjugated organic semiconductors.[1] Knowledge of solid-state molecular packing in highly organized 1D nanostructured semiconductors is critical for determining charge transport mechanisms[2] and for rational design of high-performance nano- and microelectronic devices.[3] The control of organic semiconductors on the nanoscale[4] has proven to be an extremely challenging task; however, there are a number of recent reports describing the synthesis of 1D crystalline nanowires from both p-type[5] and n-type[6] semiconductors for applications in organic field-effect transistors (OFETs).[7]

Much progress has also been made in developing 1D polymer nanostructures for a multitude of device applications.[3,8] Such 1D polymer nanostructures are of broad current interest because of the tunability of their electronic and optical properties,[9] cost-effective processability,[10] and their growing use in devices such as sensors,[11] memory units,[12] photodetectors,[13] photovoltaic cells,[14] nanolasers,[15] and OFETs.[16]

* Corresponding author. E-mail: xia@biomed.wustl.edu (Y.X.); jenekhe@u.washington.edu (S.A.J.).
[†] Department of Chemistry, University of Washington.
[‡] Department of Chemical Engineering, Stanford University.
[§] Department of Materials Science & Engineering, University of Washington.
[||] Department of Chemical Engineering, University of Washington.

(1) Hoeben, F. J. M.; Jonkheijm, P.; Meijer, E. W.; Schenning, A. P. H. J. *Chem. Rev.* **2005**, *105*, 1491–1546.
(2) (a) Curtis, M. D.; Cao, J.; Kampf, J. W. *J. Am. Chem. Soc.* **2004**, *126*, 4318–4328. (b) Coropceanu, V.; Cornil, J.; da Silva Filho, D. A.; Olivier, Y.; Silbey, R.; Bredas, J.-L. *Chem. Rev.* **2007**, *107*, 926–952.
(3) Aleshin, A. N. *Adv. Mater.* **2006**, *18*, 17–27.
(4) Nguyen, T.-Q.; Bushey, M. L.; Brus, L. E.; Nuckolls, C. *J. Am. Chem. Soc.* **2002**, *124*, 15051–15054.
(5) (a) Xiao, S.; Tang, J.; Beetz, T.; Guo, X.; Tremblay, N.; Siegrist, T.; Zhu, Y.; Steigerwald, M.; Nuckolls, C. *J. Am. Chem. Soc.* **2006**, *128*, 10700–10701. (b) Tang, Q.; Li, H.; He, M.; Hu, W.; Liu, C.; Chen, K.; Wang, C.; Liu, Y.; Zhu, D. *Adv. Mater.* **2006**, *18*, 65–68. (c) Tang, Q.; Li, H.; Song, Y.; Xu, W.; Hu, W.; Jiang, L.; Liu, Y.; Wang, X.; Zhu, D. *Adv. Mater.* **2006**, *18*, 3010–3014. (d) Kim, D. H.; Lee, D. Y.; Lee, H. S.; Lee, W. H.; Kim, Y. H.; Han, J. I.; Cho, K. *Adv. Mater.* **2007**, *19*, 678–682. (e) Briseno, A. L.; Mannsfeld, S. C. B.; Liu, X.; Xiong, Y.; Jenekhe, S. A.; Bao, Z.; Xia, Y. *Nano Lett.* **2007**, *7*, 668–675.
(6) (a) Tang, Q.; Li, H.; Liu, Y.; Hu, W. *J. Am. Chem. Soc.* **2006**, *128*, 14634–14639. (b) Briseno, A. L.; Mannsfeld, S. C. B.; Reese, C.; Hancock, J. M.; Xiong, Y.; Jenekhe, S. A.; Bao, Z.; Xia, Y. *Nano Lett.* **2007**, *7*, 2847–2853.
(7) Zaumseil, J.; Sirringhaus, H. *Chem. Rev.* **2007**, *107*, 1296–1323.
(8) Schenning, A. P. H. J.; Meijer, E. W. *Chem. Commun.* **2005**, *26*, 3245–3258.
(9) Würthner, F. *Chem. Commun.* **2004**, *14*, 1564–1579.
(10) (a) Sirringhaus, H. *Adv. Mater.* **2005**, *17*, 2411–2425. (b) Katz, H. E.; Bao, Z.; Gilat, S. L. *Acc. Chem. Res.* **2001**, *34*, 359–369. (c) Dickey, K. C.; Subramanian, S.; Anthony, J. E.; Han, L.-H.; Chen, S. C.; Loo, Y.-L. *Appl. Phys. Lett.* **2007**, *90*, 244103.
(11) (a) Huang, J.; Virji, S.; Weiller, B. H.; Kaner, R. B. *J. Am. Chem. Soc.* **2003**, *125*, 314–315. (b) Hernandez, S. C.; Chaudhuri, D.; Chen, W.; Myung, N. V.; Mulchandani, A. *Electroanalysis* **2007**, *19*, 2125–2130.
(12) (a) Tseng, R. J.; Huang, J.; Ouyang, J.; Kaner, R. B.; Yang, Y. *Nano Lett.* **2005**, *5*, 1077–1080. (b) Tseng, R. J.; Baker, C. O.; Shedd, B.; Huang, J.; Kaner, R. B.; Ouyang, J.; Yang, Y. *Appl. Phys. Lett.* **2007**, *90*, 53101.
(13) O'Brien, G. A.; Quinn, A. J.; Tanner, D. A.; Redmond, G. *Adv. Mater.* **2006**, *18*, 2379–2383.
(14) (a) Berson, S.; De Bettignies, R.; Bailly, S.; Guillerez, S. *Adv. Funct. Mater.* **2007**, *17*, 1377–1384. (b) Xin, H.; Kim, F. S.; Jenekhe, S. A. *J. Am. Chem. Soc.* **2008**, *130*, 5424–5425.
(15) O'Carroll, D.; Lieberwirth, I.; Redmond, G. *Nat. Nanotechnol.* **2007**, *2*, 180–184.

10.1021/cm8010265 CCC: $40.75
Published on Web 06/18/2008

Nearly all reports on nanostructured polymer OFETs to date are of the p-channel type.[16,17] The scarcity of n-type polymer semiconductors[18] for OFETs is due largely to the fact that the majority of electron deficient (n-type) conjugated polymers do not have sufficiently high electron affinity essential for electron injection/transport in the presence of oxygen.[18b] An important exception is the n-type polymer BBL, recently shown to have high field-effect electron mobility in ambient air measurements.[19] Although it has been shown that even well-known p-type polymer semiconductors such as polythiophene and polyfluorene can exhibit n-channel OFET activity under vacuum, they become nonfunctional in the presence of oxygen or moisture.[20] Enabling the fabrication of 1D polymer OFETs capable of electron transport[21] in air remains an important goal for the realization of all-polymer complementary circuits,[22] which could offer a promising route to the miniaturization of organic electronic devices in general.

In this paper, we report the self-assembly, molecular packing, and charge transport of 1D nanobelts from the air-stable n-type polymer BBL.[19] By precisely controlling the solution-phase self-assembly of this polymer, we produced large quantities of solvent-dispersible BBL nanobelts in environmentally benign solvents such as methanol or water. Investigation of the molecular packing of polymer chains in the BBL nanobelts reveals a self-assembled motif unlike the traditional π-stacking common to currently known small organic molecules or polymer semiconductors that form 1D nanostructures.[5,6,16a] We determined that the BBL polymer chains pack face-to-face perpendicular to the long axis of the nanobelt instead of the more common face-to-face packing along a 1D nanowire axis commonly found in small organic molecules[5,6] and polymer semiconductors.[16] We subsequently fabricated n-channel field-effect transistors from an individual nanobelt and also from a network of nanobelts that exhibit electron mobilities and on/off current ratios on the order of $\sim 7 \times 10^{-3}$ cm^2 V^{-1} s^{-1} and $\sim 1 \times 10^4$, respectively. Finally, the nanobelt field-effect transistors showed unprecedented long-term stability in air unlike any other n-channel organic devices reported to date.

Experimental Section

Materials and Sample Preparation. All solvents were purchased and used as received from Aldrich. High purity (99.5+ %) methanesulfonic acid (MSA) was used for preparing polymer solutions. The BBL polymer sample used in this study was synthesized in our laboratory following previous reports.[23] The polymer sample has an intrinsic viscosity of 7.0 dL g^{-1} in MSA, corresponding to a molecular weight of 60 kDa.[24] BBL in this range of molecular weight yields electron mobilities on the order of $\sim 1 \times 10^{-3}$ cm^2 V^{-1} s^{-1} in thin film transistors.[24]

X-ray Diffraction Analysis. X-ray diffraction patterns were collected on a Bruker D-8 diffractometer with an 18kW TXS Cu rotating anode X-ray source. The incident beam passed through a single Göbel mirror and a 0.5 mm pinhole collimator, creating a focused parallel beam of Cu K-α radiation. The incident angle between the beam and sample was fixed at 5° and the beam was rastered across a sample area of 1 mm × 1 mm to improve counting statistics. Diffracted radiation was captured with a multiwire area-detector and spectra were integrated in χ over a range of 50 degrees to produce the final 2θ vs intensity plots. Absolute precision of this diffractometer is within $\pm 0.045°$ 2θ.

Transmission Electron Microscopy (TEM). The thin film morphology of BBL and the nanobelts were studied by TEM using a Phillips EM420 electron microscope at accelerating voltages of 80 and 100 kV and a camera length (L) of 95 cm. The samples for electron microscopy were prepared by floating BBL thin films from a glass substrate on a water surface and then transferred onto a copper grid. BBL nanobelts were drop cast onto copper grids from methanol dispersions.

Device Fabrication. The BBL nanobelt field-effect transistors were fabricated using bottom contact geometry. Heavily doped Si with a conductivity of 10^3 S/cm was used as a gate electrode with a 300 nm thick SiO_2 layer as the gate dielectric. Using photolithography and vacuum sputtering system (2×10^{-6} Torr), 50 nm thick gold electrodes (source and drain) with 5 nm thick Ti adhesive layer were fabricated onto the SiO_2/Si substrates. Channel lengths (L) of 10 and 20 μm and channel widths (W) of 100 and 200 μm were used for discrete transistors. However, because the BBL nanobelts do not entirely cover the channel widths, we carefully measured the active area covered by the nanobelts and based the W/L measured values on a device basis. Electrical characteristics of the devices were measured using a Keithley 4200 semiconductor parameter analyzer.

Results and Discussion

Self-Assembly of BBL into Nanobelts. BBL nanobelts were prepared from a solution by adding the protonated polymer (0.2 mg/mL) dropwise into a rapidly stirring mixture of chloroform and methanol (4:1). The chloroform serves

(16) (a) Merlo, J. A.; Frisbie, C. D. *J. Phys. Chem. B* **2004**, *108*, 19169–19179. (b) Gonzalez, R.; Pinto, N. J. *Synth. Met.* **2005**, *151*, 275–278. (c) Liu, H.; Reccius, C. H.; Craighead, H. G. *Appl. Phys. Lett.* **2005**, *87*, 253106. (d) Hamedi, M.; Forchheimer, R.; Inganas, O. *Nat. Mater.* **2007**, *6*, 357–362. (e) Wanekaya, A. K.; Bangar, M. A.; Yun, M.; Chen, W.; Myung, N. V.; Mulchandani, A. *J. Phys. Chem. C* **2007**, *111*, 5218–5221. (f) Babel, A.; Li, D.; Xia, Y.; Jenekhe, S. A. *Macromolecules* **2005**, *38*, 4705–4711.

(17) Ong, B. S.; Wu, Y.; Liu, P.; Gardner, S. *Adv. Mater.* **2005**, *17*, 1141–1144.

(18) (a) De Leeuw, D. M.; Simenon, M. M. J.; Brown, A. R.; Einerhand, R. E. F. *Synth. Met.* **1997**, *87*, 53–59. (b) Chabinyc, M. L.; Street, R. A.; Northrup, J. E. *Appl. Phys. Lett.* **2007**, *90*, 123508. (c) Tonzola, C. J.; Alam, M. M.; Kaminsky, W.; Jenekhe, S. A. *J. Am. Chem. Soc.* **2003**, *125*, 13548–13558. (d) Kulkarni, A. P.; Tonzola, C. J.; Babel, A.; Jenekhe, S. A. *Chem. Mater.* **2004**, *16*, 4556–4573. (e) Zhu, Y.; Alam, M. M.; Jenekhe, S. A. *Macromolecules* **2003**, *36*, 8958–8968.

(19) (a) Babel, A.; Jenekhe, S. A. *J. Am. Chem. Soc.* **2003**, *125*, 13656–13657. (b) Babel, A.; Jenekhe, S. A. *Adv. Mater.* **2002**, *14*, 371–374. (c) Babel, A.; Jenekhe, S. A. *J. Phys. Chem. B* **2002**, *106*, 6129–6132. (d) Babel, A.; Zhu, Y.; Cheng, K.-F.; Chen, W.-C.; Jenekhe, S. A. *Adv. Funct. Mater.* **2007**, *17*, 2542–2549.

(20) Chua, L. L.; Zaumseil, J.; Chang, J. F.; Ou, E. C. W.; Ho, P. K. H.; Sirringhaus, H.; Friend, R. H. *Nature* **2005**, *434*, 194–199.

(21) Zhan, X.; Tan, Z.; Domercq, B.; An, Z.; Zhang, X.; Barlow, S.; Li, Y.; Zhu, D.; Kippelen, B.; Marder, S. R. *J. Am. Chem. Soc.* **2007**, *129*, 7246–7247.

(22) (a) Sirringhaus, H.; Kawase, T.; Friend, R. H.; Shimoda, T.; Inbasekaran, M.; Wu, W.; Woo, E. P. *Science* **2000**, *290*, 2123–2126. (b) Krumm, J.; Eckert, E.; Glauert, W. H.; Ullmann, A.; Fix, W.; Clemens, W. *IEEE Electron Device Lett.* **2004**, *25*, 399–401. (c) Brown, A. R.; Pomp, A.; Hart, C. M.; de Leeuw, D. M. *Science* **1995**, *270*, 972–974. (d) Gelinck, G. H.; Geuns, T. C. T.; de Leeuw, D. M. *Appl. Phys. Lett.* **2000**, *77*, 1487–1489. (e) Clemens, W.; Fix, W.; Ficker, J.; Knobloch, A.; Ullmann, A. *Mater. Res.* **2004**, *19*, 1963–1973.

(23) (a) Arnold, F. E.; Deusen, R. L. V. *Macromolecules* **1969**, *2*, 497–502. (b) Jenekhe, S. A.; Johnson, P. O. *Macromolecules* **1990**, *22*, 4419–4429.

(24) Babel, Amit, Ph.D. Thesis, University of Washington, Seattle, 2006.

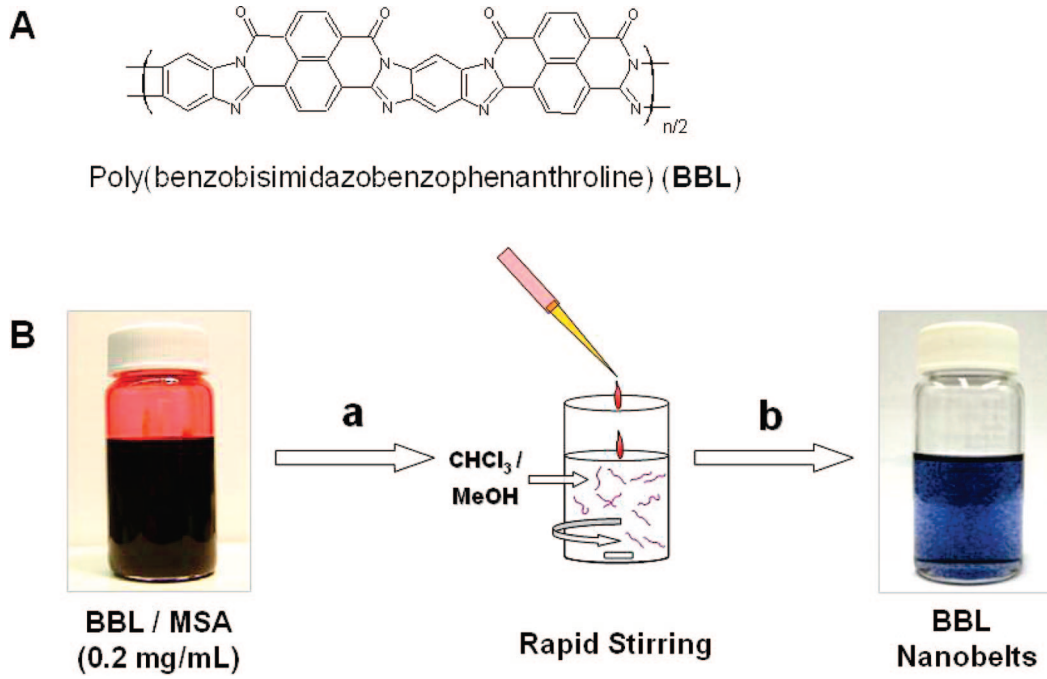

Figure 1. (A) Molecular structure of BBL, and (B) the schematic for preparing BBL nanobelts. In step "a", a BBL/methanesulfonic acid (MSA) solution (~0.2 mg/mL) is added dropwise to a rapid-stirring vial containing a $CHCl_3$/MeOH (4:1) solvent mixture. In step "b", the nanobelts are washed and centrifuged two times with deionized water. The last frame shows a vial containing an aqueous dispersion of BBL nanobelts for use in device fabrication via solution deposition.

as a weakly interacting solvent while methanol ($pK_a \approx 15$) serves as a base to deprotonate the BBL polymer chains, thus inducing the self-assembly of BBL into nanobelts. It is important to note that if a higher concentration of methanol is employed, the BBL polymer will self-assemble into larger fibers. Figure 1A shows the chemical structure of BBL and a schematic of the procedure for processing this n-type polymer into nanobelts (Figure 1B). After precipitation of the nanobelts in the $CHCl_3$/MeOH mixture, the BBL nanobelts were collected and transferred into a centrifuge tube where they were washed with methanol for 10 min at 3000 rpm, decanted, and repeated twice with water instead of methanol. The washing steps ensure that the MSA is removed from the BBL nanobelts. After the final washing step, the nanobelts were collected into a vial containing methanol and subsequently cast directly onto substrates. Other solvents such as water, ethanol, and chloroform have also been successfully used to disperse the BBL nanobelts.

Figure 2 shows a large-area optical micrograph of BBL nanobelts drop cast onto a silicon substrate from a dispersion in methanol/water (1:1) mixture. This solution deposition method is highly desirable for fabricating large-area organic electronic devices from environmentally benign alcoholic or aqueous solvents. We have routinely prepared the BBL nanobelt films from solutions of methanol, ethanol, or water. Figures 3A and 3B clearly show the "beltlike" 1D morphology as determined from TEM and SEM imaging. The nanobelts have lengths ranging from 20 μm to well over 150 μm (Figure 3C). Average widths of the nanobelts were ~200 nm to ~1 μm, while the nanobelt thicknesses (measured using AFM) were ~10−50 nm.

Molecular Packing and Structural Characterization. An important step in developing new device technologies is to obtain knowledge of the structure−property relationships of organic semiconductors at all length scales.[25–28] To acquire a better understanding of the detailed morphology, one should investigate the molecular packing and orientation of polymer chains[26,27] at nanoscale domains. Diffraction experiments on BBL thin films were previously performed by Song et al. who found that the BBL polymer forms an orthorhombic unit cell with lattice parameters of $a = 7.87$, $b = 3.37$, and $c = 11.97$ Å.[29] We performed X-ray diffraction (XRD) measurements to determine the crystal structure and molecular packing in BBL polymer films and BBL nanobelts. Figure 4A shows XRD spectra of both a nanobelt film and a standard BBL film. A strong Bragg reflection and its corresponding second order peak (200) for the BBL nanobelts are observed at $2\theta = 11.15$ and 23.28° and correspond to a *d*-spacing of 7.93 Å. Another distinctive diffraction peak is observed at $2\theta = 26.68°$, corresponding to a *d*-spacing of 3.36 Å. These two spacings are in good agreement with the previously measured lattice constants along a- and *b*-axis of the unit cell. The absence of a peak corresponding to the *c*-axis suggests that the BBL nanobelts predominantly lie on the support with the *c*-axis in the substrate plane.

We investigated the morphology of BBL thin films via TEM to identify the crystallinity and chain packing so that we may establish a comparative marker for *d*-spacing

(25) Murphy, A. R.; Frechet, J. M. J. *Chem. Rev.* **2007**, *107*, 1066–1096.
(26) DeLongchamp, D. M.; Sambasivan, S.; Fischer, D. A.; Lin, E. K.; Chang, P.; Murphy, A. R.; Fréchet, J. M. J.; Subramanian, V. *Adv. Mater.* **2005**, *17*, 2340–2344.
(27) DeLongchamp, D. M.; Kline, R. J.; Lin, E. K.; Fischer, D. A.; Richter, L. J.; Lucas, L. A.; Heeney, M.; McCulloch, I.; Northrup, J. E. *Adv. Mater.* **2007**, *19*, 833–837.
(28) Cornil, J.; Beljonne, D.; Calbert, J. P.; Bredas, J. L. *Adv. Mater.* **2001**, *13*, 1053–1067.
(29) Song, H. H.; Fratini, A. V.; Chabinyc, M.; Price, G. E.; Agrawal, A. K.; Wang, C. S.; Burkette, J.; Dudise, D. S.; Arnold, F. E. *Synth. Met.* **1995**, *69*, 533–535.

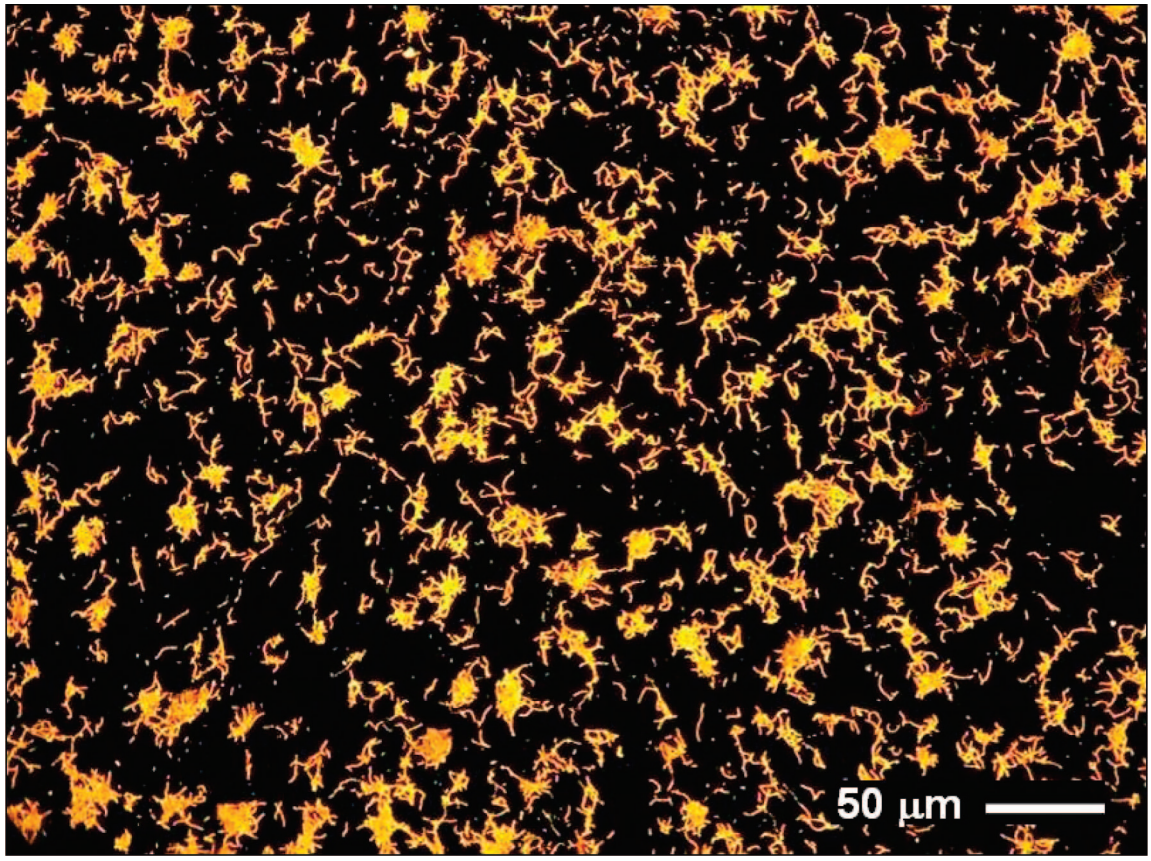

Figure 2. A large-area dark-field optical micrograph of BBL nanobelts cast from a methanol/water (1:1) solution onto a silicon substrate.

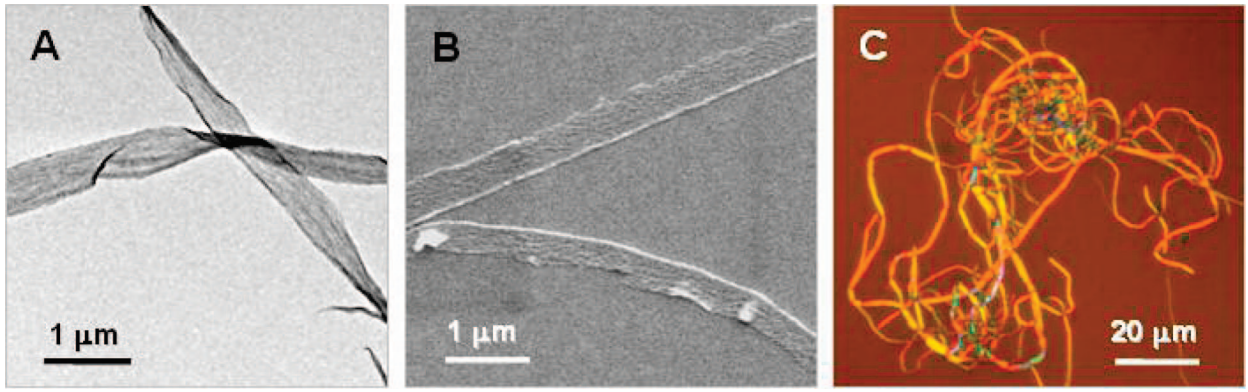

Figure 3. Representative BBL nanobelts imaged via (A) TEM, (B) SEM, and (C) an optical microscope. The widths of BBL nanobelts ranged from ~200 nm to ~1 μm and the lengths ranged from ~20 to ~150 μm. The average thickness of the nanobelts ranged from ~10 to ~50 nm.

analysis. Figure 5A shows a TEM image of the morphology of a standard BBL thin film that is polycrystalline in which the size of the individual grains ranges from 25 to 150 nm. The inset gives the diffraction pattern, showing well-resolved Debye rings with the most intense reflection corresponding to a *d*-spacing of 3.4 Å, which is in agreement with the (010) reflection measured from the XRD diffraction. Figure 5B shows a TEM image of a BBL nanobelt network and the corresponding electron diffraction pattern (inset). Similar to the standard thin-film diffraction in the inset of Figure 5A, the TEM diffraction pattern of the nanobelt network also shows diffraction rings which indicates that the individual nanobelts are polycrystalline. The Debye rings are broader compared to those obtained from the thin-film sample, indicating a slightly lower degree of crystalline order in the nanobelt network. Nevertheless, the (010) reflection clearly shows well-resolved diffraction rings with a *d*-spacing of ~3.45 Å. Interestingly, the electron diffraction of a single BBL nanobelt shown in Figure 5C exhibits distinctive intensity maxima (arcs) within the (010) Debye ring (*d*-spacing of ~3.45 Å), indicating that the crystal grains, which comprise the BBL nanobelt, are predominantly oriented with their *b*-axis perpendicular to the long axis of the nanobelt. In the unit cell for a thin film, the BBL polymer chains are π-stacked along the *b*-axis.[29,30] The assumption that the BBL nanobelts grow in the same structure as the BBL thin film, therefore, leads to the somewhat surprising conclusion that

(30) Song, H. H.; Kim, D. Y. *Bull. Korean Chem. Soc.* **1998**, *19*, 516–518.

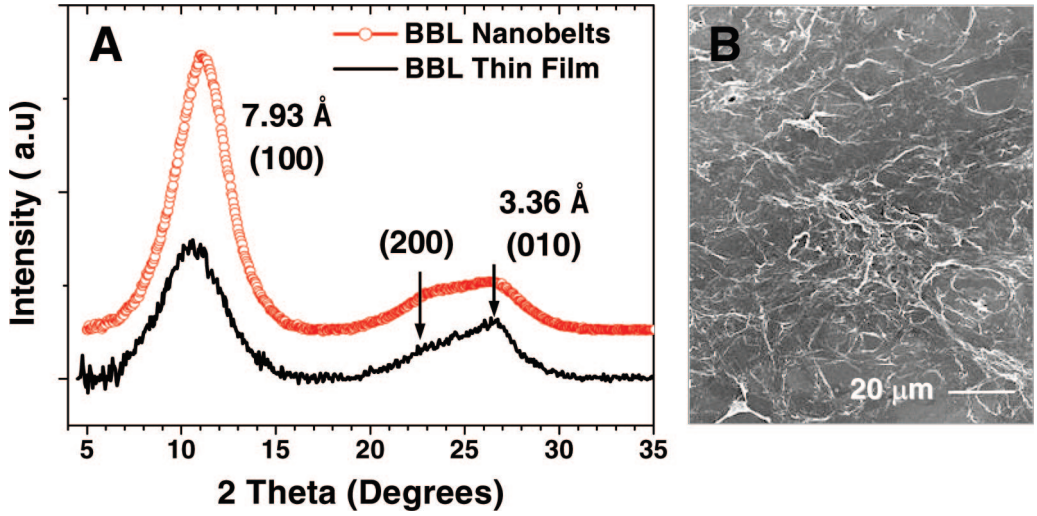

Figure 4. (A) X-ray diffraction pattern of a film of BBL nanobelts and a standard BBL thin film. (B) SEM image of the corresponding BBL nanobelt film used in the XRD measurement.

the $\pi-\pi$-stacking direction in the BBL nanobelts does not correspond to the long axis of the nanobelt. In most nanobelts composed of small planar organic molecules,[5,6] the molecules pack face-to-face along the long axis direction.

On the basis of the XRD and TEM results, we propose a unit cell for the BBL nanobelts as found in the thin films (Figure 6A). The *a* and *b* lattice parameters that were determined from our XRD experiments are, as previously mentioned, in good agreement with published unit cell parameters.[29,30] The *c*-axis unit cell is the corresponding literature value that was incorporated into our model.[29,30] Figure 6B shows an illustration of the proposed preferred orientation of BBL polymer chains in the nanobelts. It was previously suggested that the molecular plane of BBL polymer chains is oriented perpendicular to the substrate surface, agreeing with the model we propose in Figure 6B.[30] On the basis of XRD experiments, TEM diffraction on thin films and nanobelt networks, and single nanobelt diffraction patterns, we concluded that BBL polymer chains are (i) oriented parallel to the long axis of the nanobelt (i.e., the *c*-axis), and (ii) stacked face-to-face along the "width" of the nanobelt (*b*-axis). On the basis of measurements of nanobelt morphology (thickness = 10−50 nm, width = 200−1000 nm), we estimated that the thickness of each nanobelt corresponds to 13−63 layers of BBL polymer chains, and a width corresponds to 590−3000 polymer chains packed face-to-face across a BBL nanobelt. From a molecular weight of ~60 kDa for the BBL sample employed in this study, and incorporation of the *c*-axis unit cell parameter (11.97 Å),[29,30] one can estimate the average length of a polymer chain to be about 200 nm. Such a length is approximately 50−100 times shorter than the channel length (*L*) of our source-drain electrodes.

Effect of Chain Orientation on Diffraction and Factors Governing Self-Assembly. As a comparison, we want to point out that the unique 1D packing of BBL chains within nanobelts is in contrast to the molecular organization of polymer chains in poly(3-hexylthiophene) (P3HT) nanowires.[16a,31,32] We note that if BBL polymer chains are parallel to the nanobelt axis (i.e., along the *c*-axis), the reflection arcs will appear at the equator of a reflection sphere (as in Figure 5C). If, however, the molecular plane of the polymer chains are oriented face-to-face along the fiber axis, then the [010] reflection arcs would appear along the meridian of a reflection sphere.[31] This type of molecular packing has been previously demonstrated with P3HT nanowires.[16a,31,32] There are several important factors that govern the self-assembly process of molecules (whether they are small organic molecules as previously mentioned, or P3HT polymer chains) along a nanowire axis. For example, the factors governing the self-assembly of P3HT (either in 1D wires or 2D sheets) are (i) $\pi-\pi$ stacking,[31,32] (ii) alkyl-chain hydrophobic interactions (side-chain effects),[33] and (iii) solvent effects.[32] These factors have also been attributed to the self-assembly of 1D organic nanobelts consisting of small organic molecules.[5,6] However, additional factors that may contribute to 1D self-assembly in small organic semiconductors include heteroatom−heteroatom intermolecular interactions[1,5e] and hydrogen bonding.[1,9]

In the case of BBL nanobelts, the unusual anisotropic 1D self-assembly of polymer chains into nanobelts can be attributed to the very rigid and planar molecular backbone that enables the polymer chains to form intermolecular $\pi-\pi$ interactions with extraordinary strength.[23,24,34] J. E. Mark and co-workers[34] developed a model for the molecular packing of polymer chains in BBL by means of empirical

(31) Ihn, K. J.; Moulton, J.; Smith, P. *J. Polym. Sci., Part B: Polym. Phys.* **1993**, *31*, 735–742.
(32) (a) Kim, D. H.; Han, J. T.; Park, Y. D.; Jang, Y.; Cho, J. H.; Hwang, M.; Cho, K. *Adv. Mater.* **2006**, *18*, 719–723. (b) Kim, D. H.; Park, Y. D.; Jang, Y.; Kim, S.; Cho, K. *Macromol. Rapid Commun.* **2005**, *26*, 834–839.
(33) (a) Malik, S.; Nandi, A. K. *J.Polym. Sci., Part B: Polym. Phys.* **2002**, *40*, 2073–2085. (b) Kim, D. H.; Park, Y. D.; Jang, Y.; Yang, H.; Kim, Y. H.; Han, J. I.; Moon, D. G.; Park, S.; Chang, T.; Chang, C.; Joo, M.; Ryu, C. Y.; Cho, K. *Adv. Funct. Mater.* **2005**, *15*, 77–82. (c) Yang, H.; Shin, T. J.; Bao, Z.; Ryu, C. Y. *J. Polym. Sci., Part B: Polym. Phys.* **2007**, *45*, 1303–1312. (d) Mena-Osteritz, E.; Meyer, A.; Langeveld-Voss, B. M. W.; Janssen, R. A. J.; Meijer, E. W.; Bauerle, P. *Angew. Chem., Int. Ed.* **2000**, *39*, 2680–2684.

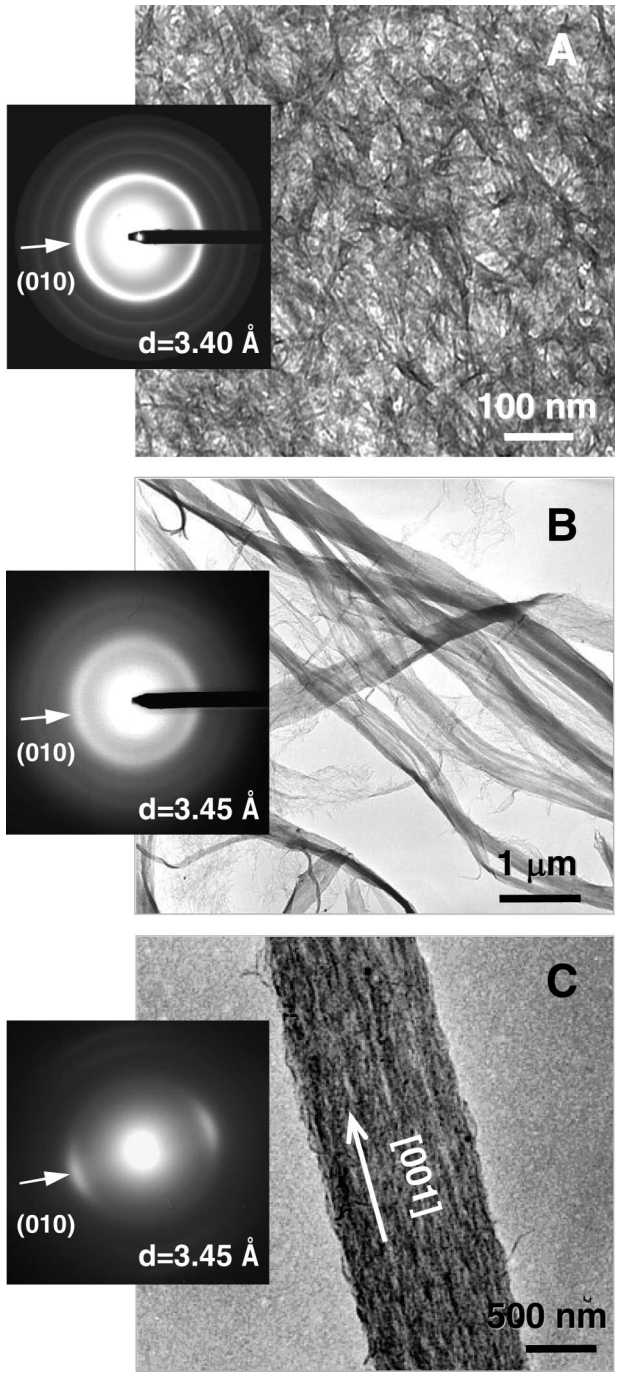

Figure 5. Representative TEM images of a (A) BBL thin film, (B) BBL nanobelt network, and (C) individual BBL nanobelt. The insets are the corresponding selected area electron diffraction patterns. The intense BBL thin-film diffraction from (A) serves as the standard marker for indexing the first diffraction ring (corresponding to $b = 3.4$ Å). A notable observation from (C) is the textured morphology of the polymer chains that are aligned along the [001] direction or the long axis of the nanobelt, thus demonstrating the extent of orientation.

force-field calculations. It was found that van der Waals contributions to the total binding energy were more significant to the overall intermolecular energy associated in BBL polymer chain packing than the Coulombic (i.e., electrostatic) contributions. Furthermore, an interchain distance of ~3.3 Å along the *b*-axis was predicted and a total intermolecular interaction energy of ~160 kJ/mol was calculated.[34] It was also suggested that because of the strong intermolecular interactions, the BBL chains may very well begin the aggregation and 1D self-assembly, to a certain degree, in their acidic solutions.[34] An important question is why BBL polymer chains pack face-to-face perpendicular to the nanobelt axis instead of along the nanobelt axis like in the case of P3HT? We previously mentioned that self-assembly in P3HT nanowires is suggested to be driven by several factors such as π-stacking,[31,32] side-chain effects,[33] and solvent effects.[32] Unlike the case of P3HT,[33d] the BBL chains are unable to fold into lamella (because of the planar and rigid backbone). We should mention, however, that the molecular plane of BBL chains are not entirely perpendicular to the surface substrate as shown in the illustration from Figure 6B, and it is likely that there is some degree of azimuthal tilting from the polymer backbone along the *b*-axis. Therefore, the most significant factor contributing to the unusual 1D self-assembly of BBL into nanobelts is likely the rigid and planar backbone.

Electrical Characterization. All electrical measurements were performed in ambient conditions and ambient light using a standard probe station. Saturation-regime mobilities were calculated by the equation, $I_{DS} = (WC_i\mu/2L)(V_G - V_T)^2$, where I_{DS} is the drain-source current, C_i is the capacitance of the dielectric, V_G is the gate voltage, μ is the mobility, and V_T is the threshold voltage. W and L are the channel width and length of the organic semiconductor. Figure 7A shows a single BBL nanobelt bridging a source and drain electrode. The output curve (Figure 7B) exhibits well-resolved saturation currents with excellent modulation as the gate voltage is increased from 0 to 80 V. The onset of the current output curves all show characteristics of contact resistance. This effect is often observed with bottom contact source-drain electrodes and can be eliminated or reduced by employing a top-contact configuration.[7] Figure 7C shows a plot of the log and square-root of drain current as a function of gate voltage (V_G). The transfer curve shows an increase in current by more than 4 orders of magnitude when the voltage is ramped from −10 to 50 V. The square-root of drain current follows the square law and the fitting line used for calculating mobility fits the data over a wide range of gate voltage values. Results from a single nanobelt n-channel transistor showed an electron mobility of 7×10^{-3} cm^2 V^{-1} s^{-1}, a threshold voltage of 11.2 V, and an on/off current ratio of $\sim 1 \times 10^4$. These results are comparable to those reported for p-channel OFETs based on single polymer nanowires.[16a–c] Therefore, this may open the possibility of fabricating all-polymer nanowire integrated circuits.

We also fabricated n-channel transistors from a network of BBL nanobelts across source-drain electrodes (Figure 7D). Figure 7E shows the output curves of a nanobelt network device, whereas Figure 7F shows the transfer and square-root characteristics. From the slope of the linear region, a mobility of 4×10^{-3} cm^2 V^{-1} s^{-1}, a threshold voltage of 11.9 V, and an on/off current ratio of $\sim 1 \times 10^4$ was calculated. These results are among the best for single and nanowire network devices.

Air Stability of BBL Devices. The BBL nanobelt network transistors were fabricated and characterized under ambient conditions and they have shown stable and reproducible performance in air for well over 6 months as seen in the

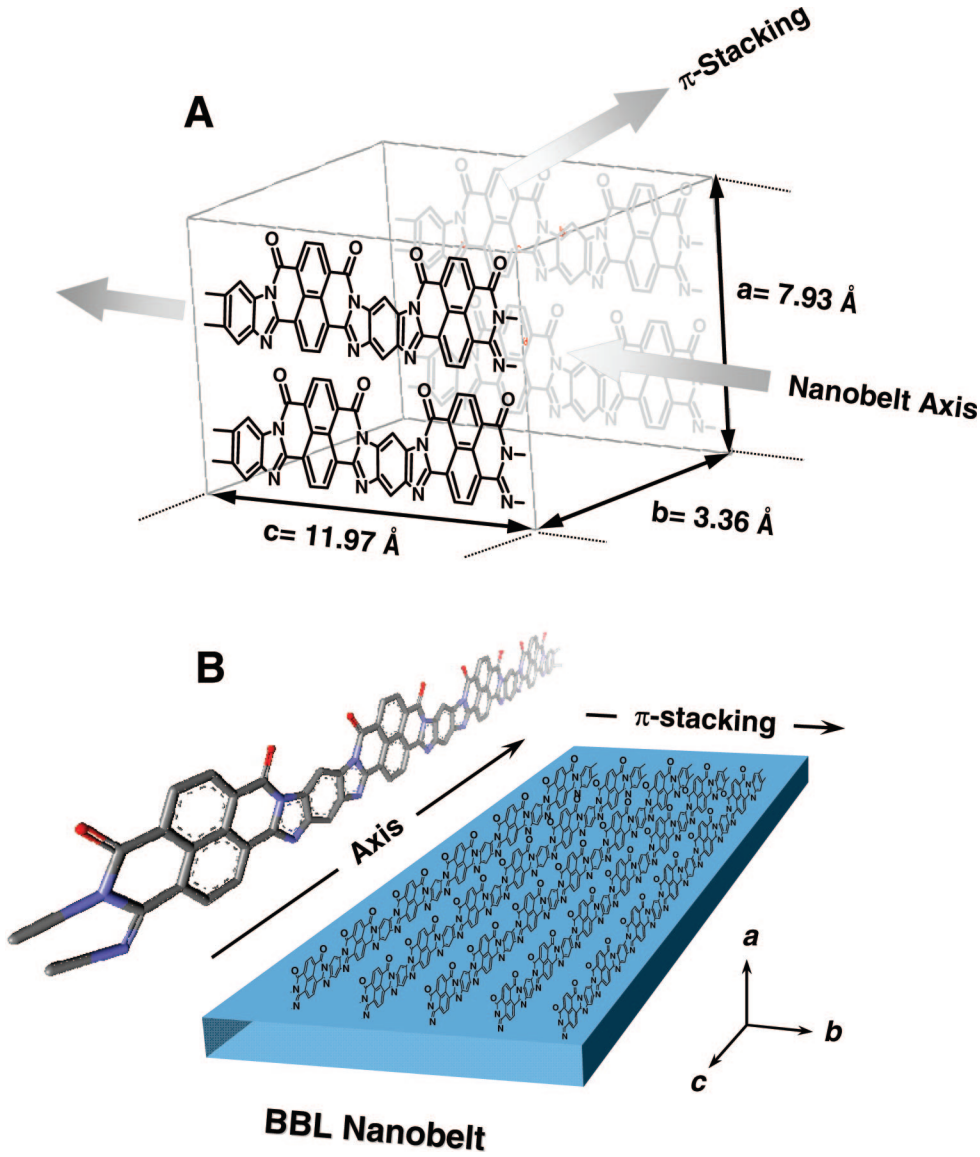

Figure 6. (A) Schematic representation of the molecular arrangement of BBL polymer chains in the orthorhombic unit cell with indicated crystallographic axis directions. (B) Perspective illustration of the molecular packing of BBL polymer chains within a nanobelt. The proposed arrangement of BBL polymer chains are determined from the TEM electron diffraction and XRD measurements.

plot of Figure 8A. Panels B and C in Figure 8 show the output and transfer characteristics with an overlay of the performance of the same device after 200 days. These results are among the most stable reported to date when compared to currently known n-type polymer semiconductors.[21,22] The stability of the BBL nanobelt transistors arise from the favorable electronic and molecular structure of the polymer as well as the morphology of the oriented polymer chains within the nanobelts. For instance, BBL has an experimental LUMO value of ~4.2 eV.[35] Such a high electron affinity is rare among polymer semiconductors and as a result, good electron injection and transport is facilitated by the low-lying molecular orbital. The polymer also has a more positive reduction potential compared to oxygen ($BBL_{(red)} = -0.4$ V; $O_{2(red)} = -0.87$ V vs SCE), and this enables "electrons" or the BBL radical anions to remain thermodynamically stable in the presence of oxygen. This is an important electronic property to possess as it is well-known that oxygen is the main reason behind stability problems with organic semiconductors in general.[18a,b] The morphology of the polymer nanobelts also contributes to the stability of the device. We recall that BBL polymer chains form very strong intermolecular contacts with interplanar distances ranging from 3.36 to 3.4 Å. As such, oxygen, which has a kinetic diameter of 3.46 Å,[36] is unlikely to diffuse into the BBL nanobelt in significant amounts. This effect has previously been shown in gas separation studies involving films of BBL and other ladder-type polymers.[36] The oriented BBL polymer chains, which are strongly interacting with one another, form a "kinetic" barrier against moisture and oxygen as well.[36] Therefore, the unique properties of BBL provide a thermodynamic and kinetic advantage for exhibiting long-term stability in the presence of oxygen.

Conclusions

We have devised a simple, high-yield, solution-phase synthesis of nanobelts from the n-type polymer semiconduc-

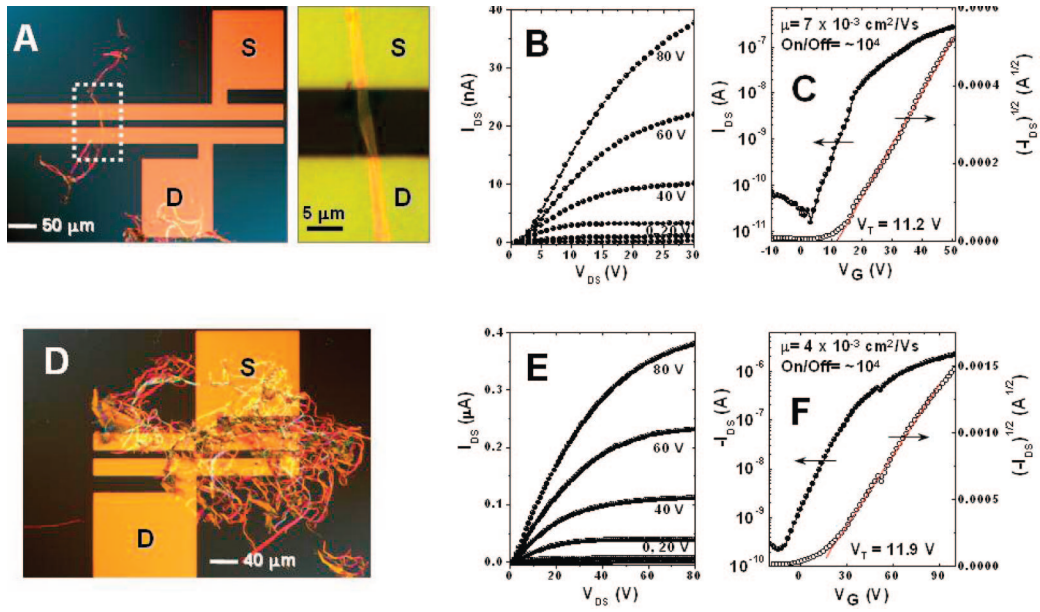

Figure 7. (A) Typical single BBL nanobelt transistor and a close-up showing the nanobelt bridging the source-drain electrodes. (B) Output characteristics showing well-resolved current−voltage saturation. (C) Corresponding transfer and square root of current characteristics. (D) Network of BBL nanobelts drop cast onto gold source/drain electrodes. (E) Output and (F) transfer/square root of current characteristics from a nanobelt transistor similar to the image shown in (D). All measurements on nanobelt transistors were performed under ambient conditions.

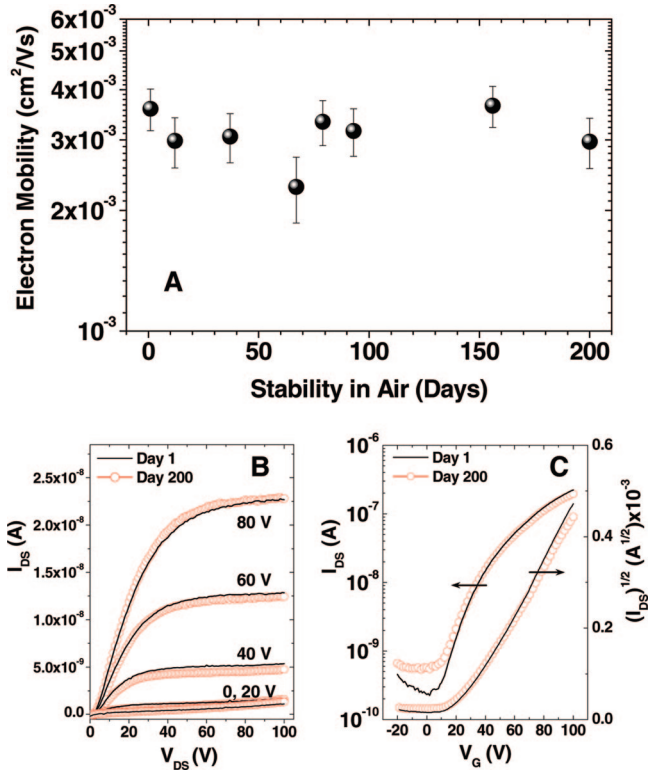

Figure 8. (A) Plot of air stability of a BBL nanobelt transistor measured in ambient laboratory conditions over a period of ~6 months. (B) Output and (C) transfer/square root of current characteristics of the actual device with an overlay after 200 days. All measurements were carried out under ambient conditions of a normal laboratory.

tor, BBL. The BBL nanobelts are dispersible in a large number of solvents including environmentally benign solvents such as methanol and water. We have found that BBL polymer chains are oriented parallel to the nanobelt axis (i.e., face-to-face, perpendicular to the nanobelt axis). This unique packing motif is unlike the reported packing of polymer chains in P3HT nanowires, where the polymer backbone packs face-to-face along the nanowire direction. We explain the unique packing in BBL nanobelts to arise from the extraordinary strength of intermolecular contacts, which is a result of the rigid and planar molecular backbone of the polymer. As a demonstration of their potential use in electronic devices, we fabricated single and nanobelt network transistors with mobilities of $(3-7) \times 10^{-3}$ cm^2 V^{-1} s^{-1} and current on/off ratios of $\sim 1 \times 10^4$. Finally, we found that the BBL devices had long-term stability in air. These results are among the most stable to date when compared to n-channel polymer transistors. We anticipate that these results will enable the production of nanoscale integrated circuits in due course.

Acknowledgment. A.L.B. acknowledges the Bell Laboratories Graduate Research Fellowship. S.A.J. acknowledges support from the NSF (CTS-0437912), the NSF STC-CMDITR (DMR-0120967), and the Air Force Office of Scientific Research (AFOSR; Grant F49620-03-1-0162). S.C.B.M. acknowledges a postdoctoral fellowship from the Deutsche Forschungsgemeinschaft (DFG; Grant MA 3342/1-1). Z.B. acknowledges support from the Stanford NSF-MRSEC Center for Polymeric Interfaces and Macromolecular Assemblies (DMR-0213618) and the NSF Solid State Chemistry Program. We thank Dr. Amit Babel for providing the TEM diffraction data on BBL thin films, and F. S. Kim and Professors Kilwon Cho and Hyun Hoon Song for stimulating discussions.

CM8010265

(34) Nayak, K.; Marks, J. E. *Makromol. Chem.* **1986**, *187*, 1547–1550.
(35) (a) Quinto, M.; Jenekhe, S. A.; Bard, A. J. *Chem. Mater.* **2001**, *13*, 2824–2832. (b) Wilbourn, K.; Murray, R. W. *J. Phys. Chem.* **1988**, *92*, 3642–3648. (c) Alam, M. M.; Jenekhe, S. A. *Chem. Mater.* **2004**, *16*, 4647–4656.
(36) Zimmerman, C. M.; Koros, W. J. *Polymer* **1999**, *40*, 5655–5664.